



Multi-Century Spring Flood Reconstruction in Eastern Boreal Canada from Novel Application of Wood-Cell Anatomy

Alexandre F Nolin^{1,2} , Jacques C Tardif², France Conciatori², David M Meko³ and Yves Bergeron¹

¹ Forest Research Institute, University of Quebec A-T, Canada; ² Center for Forest Interdisciplinary Research, University of Winnipeg, Canada; ³ Laboratory of Tree Ring Research, University of Arizona, USA

Background and aims

While global warming is associated with reduced snow cover, Canada has become increasingly prone to spring snowmelt flooding in recent decades (Bush & Lemmen, 2019). Hydrological projections suggest increased winter runoff and earlier spring flooding, but how projected changes in climate will affect the frequency and magnitude of flooding is still uncertain (Gaur *et al.*, 2018).

To complement the short instrumental hydrological data for boreal Canada, conventional dendrochronological approaches are limited by the low dependence between tree growth and water availability (Boucher *et al.* 2011). In boreal environment the study of flood rings in ring-porous trees periodically flooded has recently demonstrated linear relationships between the cross-sectional lumen area and number of earlywood (EW) vessels and the magnitude of flooding (Kames *et al.* 2016 ; Fig. 1).

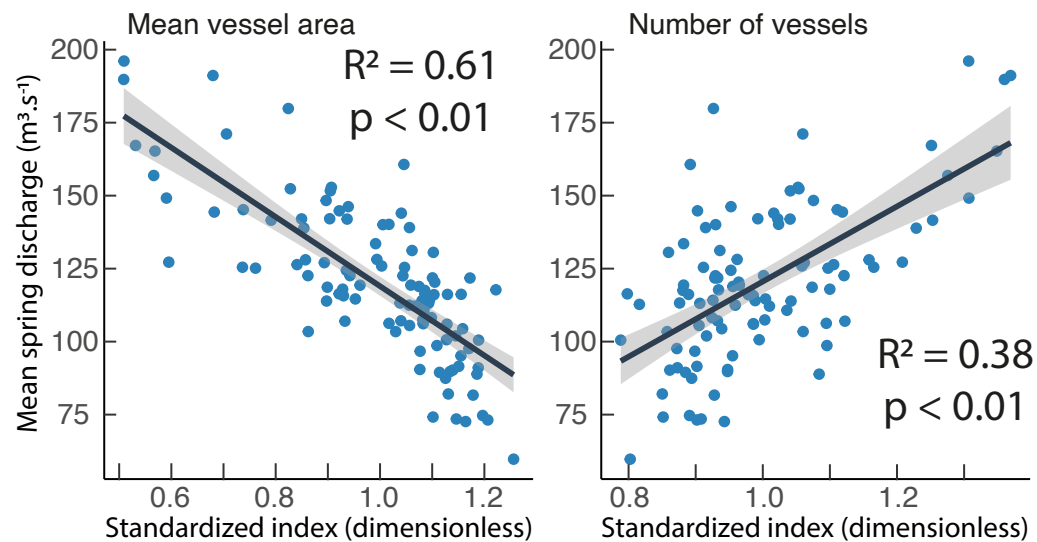
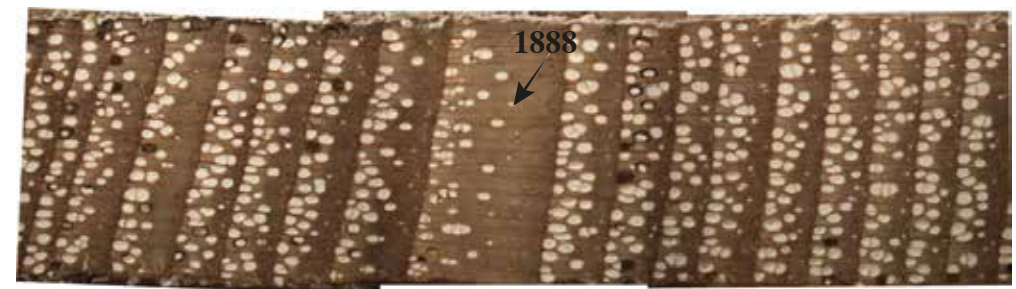


Fig. 1: Updated Kames *et al.* 2016 relationship between mean cross-sectional lumen area, number of EW vessels chronologies of *Fraxinus nigra* and spring discharge, 1915-2016.



Fig. 2: *Fraxinus nigra* tree flooded in spring 2019, Lake Duparquet. The core from this tree shows an example of the 1888 flood ring. The vessels appear white as they were rubbed with chalk.



Methods

We have developed 12 anatomical chronologies of tree rings of 43 *Fraxinus nigra* trees growing in the Lake Duparquet floodplain (Fig. 2). Using a high-resolution image acquisition technique, the vessel shapes of the EW were digitized for each year to produce annual series of geometrical parameters (size, number, width, among others) (Fig. 3). Chronologies were then used as predictors in a principal component regression model to reconstruct mean spring discharge.

Then, we studied the temporal stability of the reconstructed spring discharge and investigated the relationships with climate and atmospheric teleconnection indices to understand the climatic mechanisms associated with spring flooding.

We also collected 944 *F. nigra* samples from 4 watersheds adjacent of Lake Duparquet to investigate for spatial coherency of flood-ring signal between natural, and regulated river, and an unflooded control site. For each year, the presence/absence of flood-ring as well as any noticeable changes in the annual size and number of earlywood vessels were noted and used as semi-quantitative indicators of spring floods.

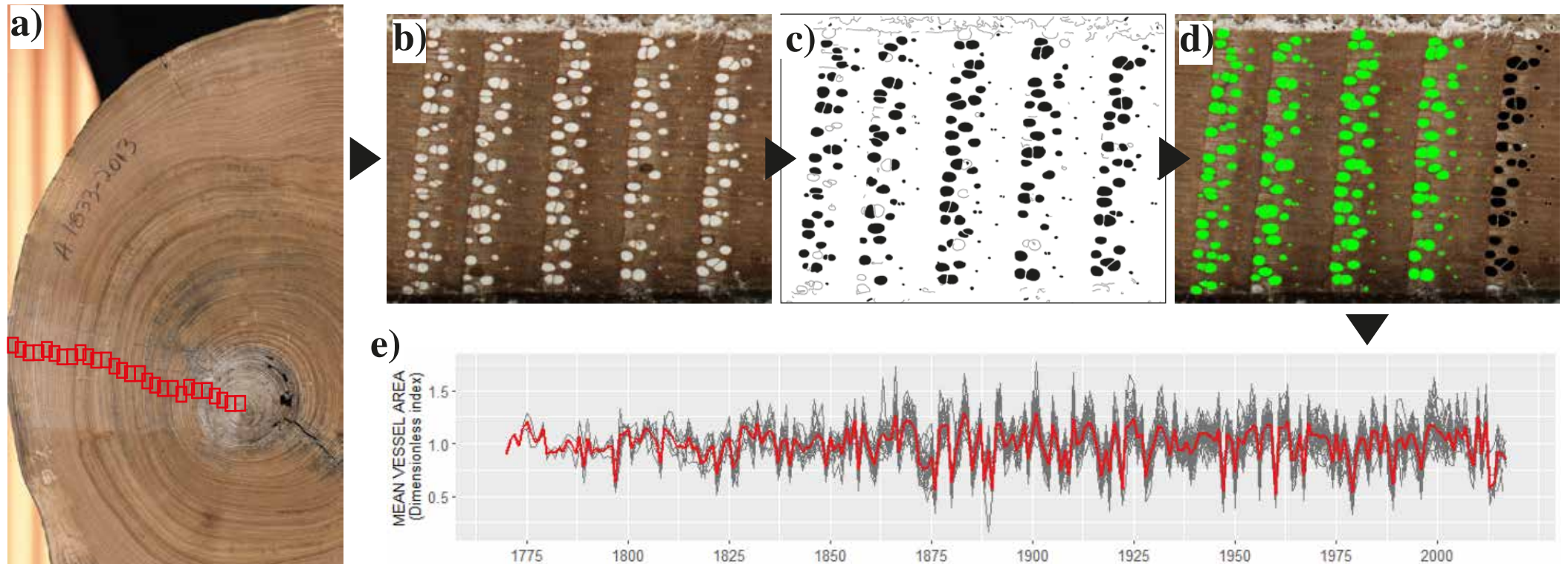


Fig. 3: a) Vessel scanning process use to produce b) high resolution image acquired at x20 magnification in 1600x1200 dpi; c) automatic detection of vessels by Canny's algorithm (*Canny, 1986*) under ImageJ2x; d) final detection after manual correction: image ready to be analyzed with WinCell software to produce e) dendroanatomical time series, here an example of the mean cross-sectional lumen area of EW vessel.

1. Reconstruction of spring discharge

The reconstruction spans 1770 to 2016 and captured 68.5% of the spring discharge variance over the calibration period (1915-2016) with a mean absolute error of $12\text{m}^3/\text{s}$ (Fig. 4a). Among the 12 dendroanatomical chronologies developed, the mean cross-sectional vessel lumen area and the number of vessels contributed most of the explained variance (PC1 = 63.87%). The majority of high discharge years are recorded after the 1870's and the highest discharges are recorded after 1950 (1960 and 1979). The majority of the low discharges are also recorded between 1850 and 1950, but the extreme minimums are in 1775, 1901 and 1958 (Fig. 4a).

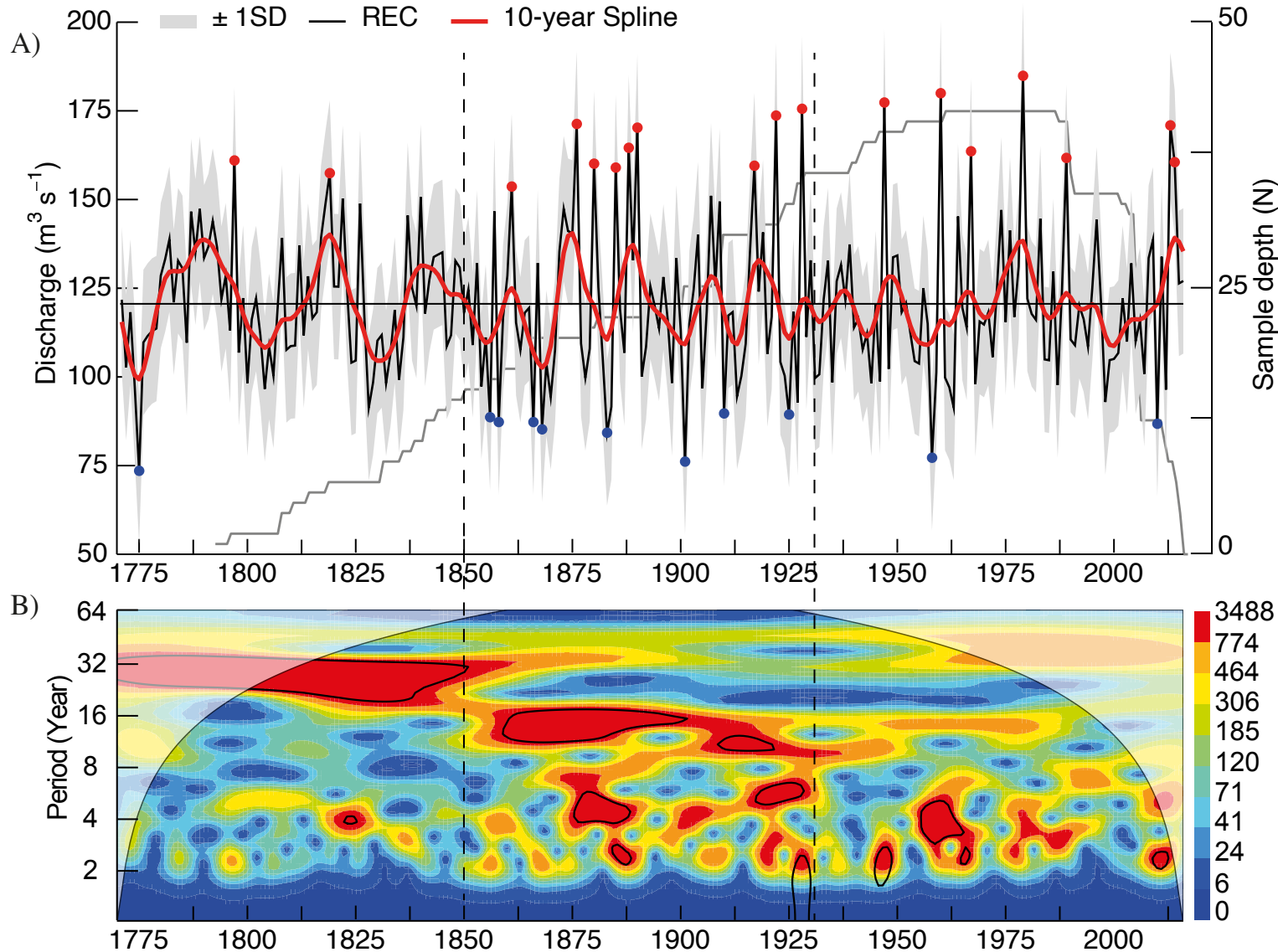


Fig. 4: A) Reconstructed spring flood. High (red dots) and low discharge years (blue dots) are extremes that exceed the thresholds ± 1.5 SD. Horizontal line is the mean ($120.60 \text{ m}^3/\text{s}$) and 10-yr spline (red curve) highlight decadal variations. B) Reconstruction decomposed into Morlet 6th power in continuous wavelet transform. Black lines encircle areas were p-value > 0.05 tested against white noise. Variance intensity range for blue (low) to dark red (high)

2. Temporal variability of spring discharge

Continuous wavelets transform reveals a non-stationary process composed of three distinct periods (Fig. 4b). An initial 30-years oscillation, stable for a 100-years period during the Little Ice Age was replaced by a pattern close to a decadal frequency starting around 1850, and evolved into a more high-frequency pattern after 1930. From this period, the temporal coherency is unclear with several patterns of high variance suggesting a change in recent variability toward a higher frequency of spring maximum (Fig. 4).

Using the linear regression of the 30 highest values of the reconstructed spring discharge, this increase in spring maximum can be quantified as $1\text{ m}^3/\text{s}$ per decade ($R^2 = 0.334$, $p < 0.001$). Correlations between our reconstruction and ice-breakup dates of Lake Duparquet recorded since 1960 also reveal that spring maximums occurs preferentially during years with the latest ice-breakup ($r = 0.493$, $p < 0.001$, 1968-2016).

3. Relationships with climate

The reconstruction is significantly correlated to previous winter (Dec), current spring mean temperature (March & April, $r = 0.30$ and 0.37 , $p < 0.001$) and total precipitation (March & April, $r = 0.14$ and 0.19 , $p < 0.001$) from 1901-2016 CRU TS 4.03 climate data (Harris *et al.* 2020 ; Fig. 5 on next page). Spatial field correlations indicated a strong and positive association with April and May snow cover extent (1966-2016 NOAA Rutgers) across much of central/eastern north Canada (**Fig. 6**). Maximum spring discharge occur during years with cold and late springs when the winter snowpack is thick.

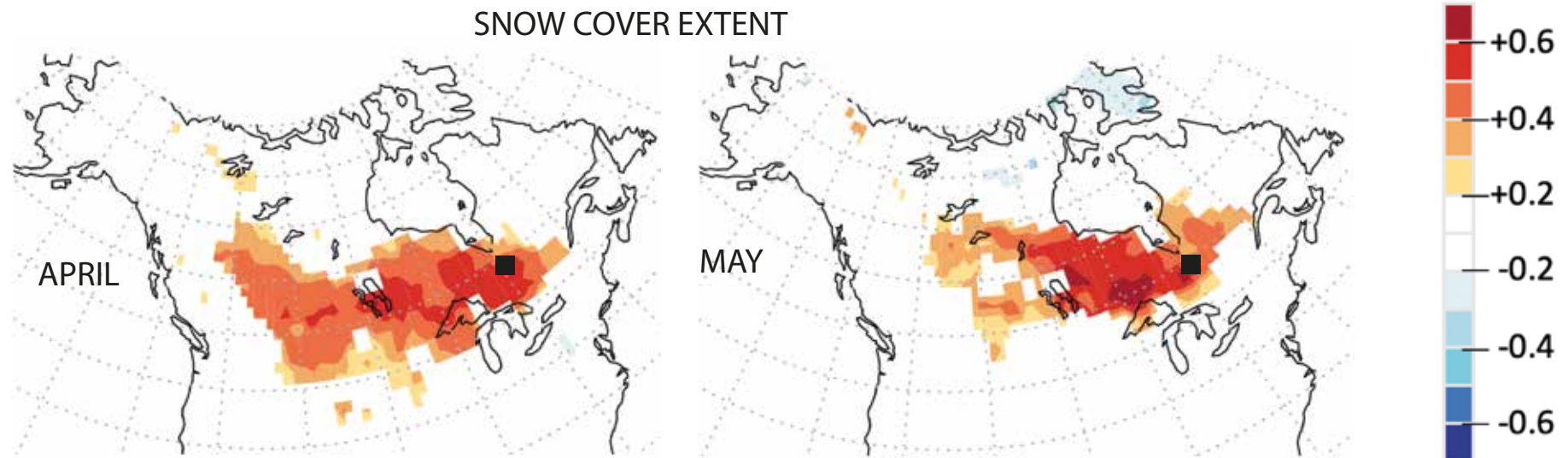


Fig. 6: Spatial field correlations between reconstructed spring discharge and 1966-2016 NOAA Rutgers snow covers provided at p .value > 0.01 level. Black square indicate Lake Duparquet location, and coefficients range from red (positive) to blue (negative correlation). Maps were obtained using the KNMI Climate explorer (<http://climexp.knmi.nl/>)

4. Associations with climate indices

Spring discharge reconstruction is also correlated to large-scale atmospheric circulation indices. The strongest monthly response to the 1900–2016 January to April El-Niño Southern Oscillation (NINO3.4, $r = -0.20$, $p < 0.05$) and to the December to February Pacific Decadal Oscillation (PDO, $r = -0.15$, $p < 0.05$; Fig. 7). No influence of the Arctic Oscillation and North Atlantic Oscillation on seasonal discharge has been detected. The Atlantic Multidecadal Oscillation was also found positively significant in April ($r = -0.14$, $p < 0.05$; Fig. 7).

The 30-years running correlations over a longer period of 1850–2002 indicate that the association with the spring (Mar–Apr–May) El-Niño and PDO indices is different over time. The association with El-Niño remains stable around -0.2 while the association with PDO, which is weaker, has diminished until it is no longer associated with spring flows from about 1960 (Fig. 8).

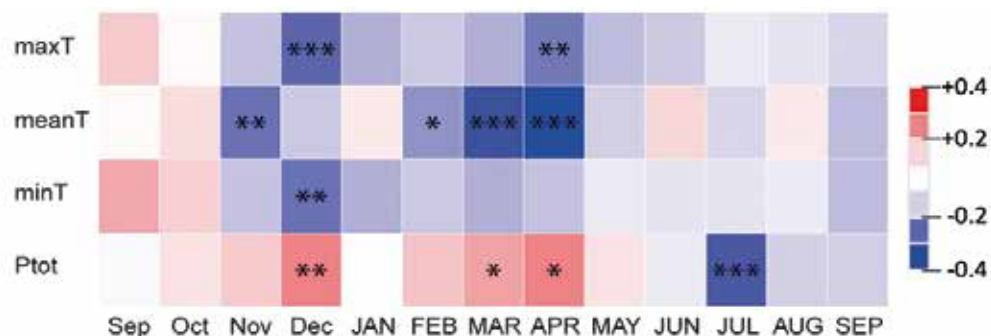


Fig. 5: Bootstrapped correlation coefficients between reconstructed spring discharge and CRU TS 4.03 monthly climate data extracted over a $0.5 \times 0.5^\circ$ landmask corresponding to Lake Duparquet. The tags *, ** and *** respectively indicates p-value < 0.05 , < 0.01 and < 0.001 level.

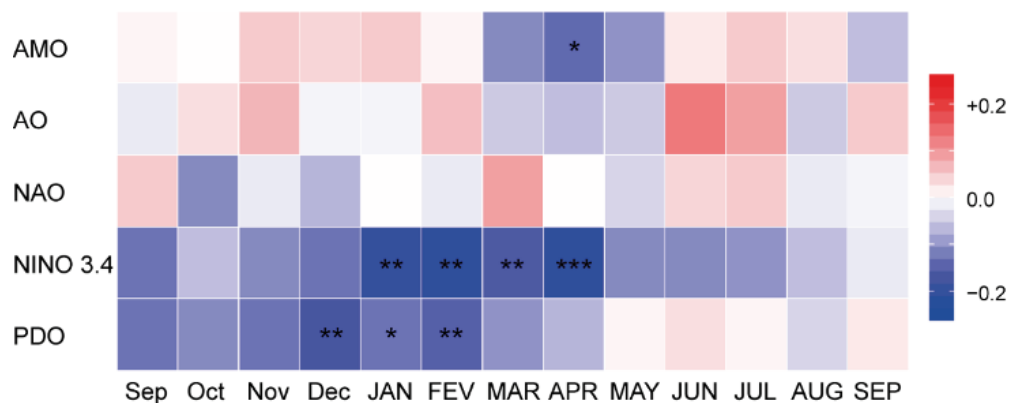


Fig. 7: Bootstrapped correlation coefficients between reconstructed spring discharge and large-scale atmospheric indices for the common period 1900–2016. The tags *, ** and *** respectively indicates p-value < 0.05 , < 0.01 and < 0.001 level.

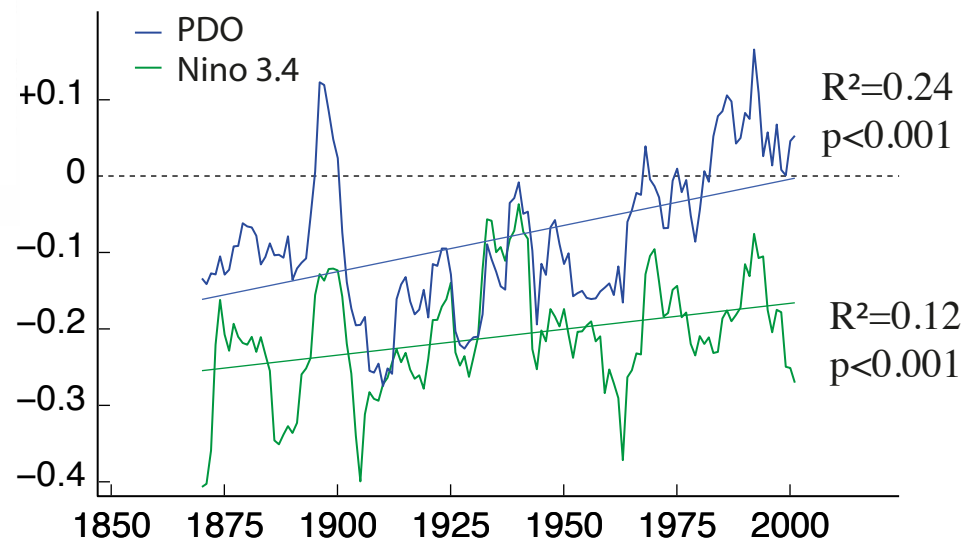
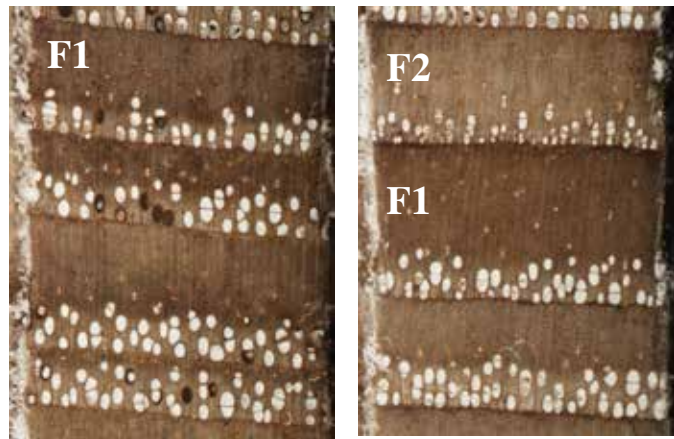


Fig. 8: Bootstrapped 10-years running correlations between reconstructed spring discharge and spring Nino3.4 and PDO indices over the 1850–2002 period. Climate indices downloaded from <http://psl.noaa.gov/>

5. Spatial association among watersheds

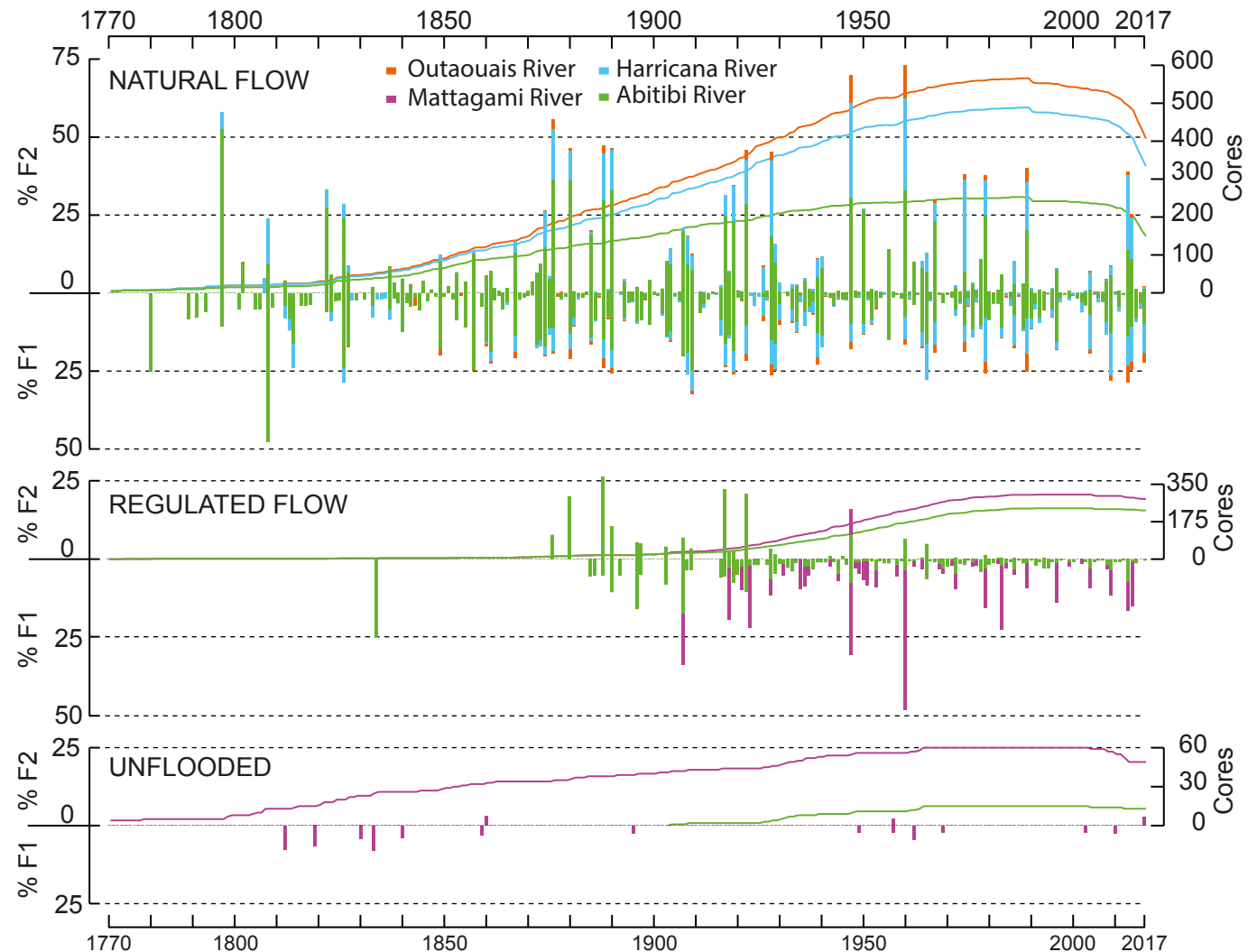
Flood-ring occurrences in the 944 samples collected in watersheds adjacent to Duparquet also provide comparable flood timing and magnitude across the 1771-2016 period. The two flood ring index that we developed are F1 (noticeable decrease in single vessel area and increase in number of vessels) and F2 (clearly distinguishable flood ring as previously described in *F. nigra* by Kames *et al.*, 2016) (Fig. 9).

In natural rivers, F1 and F2 series correlate well independently with the reconstructed spring discharge of Lake Duparquet ($r = 0.63$ and 0.67 , $p < 0.001$) and merging both indices increase the correlation to $r = 0.74$. In dam-regulated rivers, the association is weaker ($r = 0.40$; $p < 0.001$) mainly because the river basins share essentially the highest discharge years. Before the two periods of dam constructions in the 1910's and 1920's (CEHQ, 2019), the sample replication is very low, leading to almost no signal to compare with our reconstructions. The 59 trees from unflooded areas sampled as a control demonstrate no significant pattern of anatomical modification (Fig. 10).



▲ **Fig. 9:** Examples of flood-ring classes F1 and F2 in *Fraxinus nigra* wood pictures. x20 magnification.

Fig. 10: Flood-ring abundances in samples ordered by flowing regime of the rivers. Histograms pointing up are for «F2» rings, histogram pointing down are for «F1» rings. Colors are different watersheds, and sample depth for each watershed are displayed in background of each panel. ▶



Take home messages

1. *Fraxinus nigra* dendroanatomical series show a direct and robust relationship to spring discharge in a boreal environment. In particular the chronologies of number and mean cross-sectional lumen area of the EW vessels, allow excellent performances in dendrohydrological reconstruction of a boreal environment.
2. The reliability of the reconstruction support the increase in flooding frequency and magnitude since the late 1700's. Such pattern was already evidenced by numerous reconstruction in northern Québec e.g. Tardif & Bergeron, 1997; Boucher *et al.* 2010.
3. The strong spatial correlation of spring discharge in Lake Duparquet with snowy winters, early thaw and rainy springs across east-central Canada, support atmospheric forcing on inter-annual hydroclimatic variability.
4. Warm and wet air from Pacific-South Ocean (El-Niño) are associated with early spring and small floods, while cold and dry air masses (La-Niña) correlate to late thaw and high spring floods in Lake Duparquet. The weak influence of PDO over El-Niño is coherent with the documented change in PDO around the 1850s, which accentuates the inflow of wet and hot air masses from the mid-tropical ocean (ENSO) lowering the outflow of cold and dry Arctic air masses (AO and NAO) over the north-eastern Quebec (Girardin and Sauchyn, 2006 ; Boucher *et al.* 2010).
5. The occurrences of flood rings in natural flow watersheds are very consistent with the reconstruction of spring flows in Lake Duparquet. The semi-quantitative use of flood rings might be a complement or alternative to time-consuming image analysis if the number of samples is large enough ?

Conclusion

This study used a new tool for high-resolution signal acquisition of past spring flooding in the tree-ring anatomy of trees growing in flood-prone areas in a boreal watershed. We provide a unique and new high-resolution evidence of increased flooding since the end of the Little Ice Age that likely reflects an increase in snow cover over east-central Canada influenced by large-scale ENSO and PDO regulations.

This is a lightning overview of my projet, that is why I will remain fully available to answer questions on the chat on Wed, 06 May, 14:00–15:45 and by mailbox at alexandreflorent.nolin@uqat.ca for any additional information or materials. "Vive la Dendro". Alex.

Acknowledgements

This project was supported and funded by a NSERC-CRD grant involving funding supports listed in the logos (see below). We thank the entire FERLD team and D. Charron for precious support during field work, as well as field assistants C. Ducros, I. Gareau, S. Hebert & C. Lavelle. We thank J.R. Robson & H. Scwhartz for precious laboratory assistance, and a special thanks to G. Kayahara & L. Hildebrandt (Ontario Forest Services), M. Girardin (CFL) and M. Desrochers (UQAM) for forest maps and ground logistics.



References

- Boucher, E., Ouarda, T. B. M. J., Bégin, Y., & Nicault, A. (2011). Spring flood reconstruction from continuous and discrete tree ring series. *Water Resources Research*, 47(7). <https://doi.org/10.1029/2010WR010131>
- Bush, E., & Lemmen, D. S. (2019). Canada's Changing Climate Report. <http://www.changingclimate.ca/CCCR2019>
- Canny, J. (1986). A Computational Approach to Edge Detection. *IEEE Transactions on Pattern Analysis and Machine Intelligence*, PAMI-8(6), 679–698. <https://doi.org/10.1109/TPAMI.1986.4767851>
- Centre d'Expertise Hydrique du Québec (CEHQ). (2019). [in French] Répertoire des barrages. Ministère de l'Environnement et de la Lutte contre les Changements climatiques. Gouvernement du Québec, Ottawa. Available at <https://www.cehq.gouv.qc.ca/barrages/default.asp> [February 12, 2020]
- Gaur, A., Gaur, A., & Simonovic, S. P. (2018). Future changes in flood hazards across Canada under a changing climate. *Water (Switzerland)*, 10(10). <https://doi.org/10.3390/w10101441>
- Girardin, M. P., Tardif, J. C., Flannigan, M. D., & Bergeron, Y. (2006). Synoptic-scale atmospheric circulation and boreal Canada summer drought variability of the past three centuries. *Journal of Climate*, 19(10), 1922–1947. <https://doi.org/10.1175/JCLI3716.1>
- Harris, I., Osborn, T. J., Jones, P., & Lister, D. (2020). Version 4 of the CRU TS monthly high-resolution gridded multivariate climate dataset. *Scientific data*, 7(1), 1-18.
- Kames, S., Tardif, J. C., & Bergeron, Y. (2016). Continuous earlywood vessels chronologies in floodplain ring-porous species can improve dendrohydrological reconstructions of spring high flows and flood levels. *Journal of Hydrology*, 534, 377–389. <https://doi.org/10.1016/j.jhydrol.2016.01.002>

Early Spring



Late Spring



Summer



Seasons in *Fraxinus nigra* stands. Lake Duparquet shores.